

# Broadband Optoelectronic Frequency Response Measurement Utilizing Frequency Conversion

Min Xue<sup>1</sup>, Minghui Lv<sup>1</sup>, Qi Wang<sup>1</sup>, Beibei Zhu<sup>1</sup>, Changyuan Yu<sup>1</sup>, *Senior Member, IEEE*,  
and Shilong Pan<sup>2</sup>, *Senior Member, IEEE*

**Abstract**—A broadband optoelectronic (O/E) frequency response measurement method utilizing photonics-based frequency conversion is proposed and experimentally demonstrated. It is characterized by a sub-kilohertz frequency resolution and a doubled measurement bandwidth compared with the RF frequency sweeping range and the working bandwidth. A carrier-frequency-shifted optical double-sideband (ODSB) signal is produced by employing a dual-drive Mach-Zehnder modulator (DD-MZM) and stimulated Brillouin scattering (SBS). Then, a photodetector (PD) under test receives and converts the optical signal into a photocurrent. By detecting the frequency up- and down-conversion components generated by the two first-order sidebands and the optical carrier, the O/E frequency responses in the low- and high-frequency regions are achieved. After stitching the two measured responses together, an O/E frequency response with a frequency range that is twice the bandwidth of the input microwave signal is obtained. In an experiment, the O/E frequency response of a commercial high-speed PD is precisely characterized with a frequency resolution up to 5.55 MHz. A frequency bandwidth of 66.8 GHz (0.1–66.9 GHz) is achieved by using a 25-GHz DD-MZM. The measured O/E frequency response is coincident with that measured by a commercial instrument.

**Index Terms**—Microwave photonics (MWP), optical variables measurement, optoelectronic (O/E) frequency response measurement, photonics-based frequency conversion, stimulated Brillouin scattering (SBS).

## I. INTRODUCTION

MICROWAVE photonics (MWP) plays an important role in many emerging fields, which enables radio over fiber [1], optoelectronic (O/E) oscillator [2], fifth-generation networks [3], and MWP radars [4], [5]. Photodetectors (PDs)

Manuscript received November 25, 2020; revised April 25, 2021; accepted May 3, 2021. Date of publication May 19, 2021; date of current version May 27, 2021. This work was supported in part by the National Key Research and Development Program of China under Grant 2017YFF0106900, in part by the National Natural Science Foundation of China under Grant 62071226 and Grant 61971372, in part by the Hong Kong Scholar Program under Grant G-YZ2S, in part by the Jiangsu Provincial Program for High-level Talents in Six Areas under Grant DZXX-034, in part by the Postgraduate Research and Practice Innovation Program of Jiangsu Province under Grant KYLX16\_0367, and in part by HK RGC GRF under Grant 15200718. The Associate Editor coordinating the review process was Zheng Liu. (*Corresponding author: Shilong Pan.*)

Min Xue is with the Key Laboratory of Radar Imaging and Microwave Photonics, Ministry of Education, Nanjing University of Aeronautics and Astronautics, Nanjing 210016, China, and also with the Department of Electronic and Information Engineering, Hong Kong Polytechnic University, Hong Kong 999077.

Minghui Lv, Qi Wang, Beibei Zhu, and Shilong Pan are with the Key Laboratory of Radar Imaging and Microwave Photonics, Ministry of Education, Nanjing University of Aeronautics and Astronautics, Nanjing 210016, China (e-mail: pans@nuaa.edu.cn).

Changyuan Yu is with the Department of Electronic and Information Engineering, Hong Kong Polytechnic University, Hong Kong 999077.

Digital Object Identifier 10.1109/TIM.2021.3079562

are the essential devices to achieve optical-to-electrical conversion in the MWP-based systems and applications. During the design of the MWP-based systems, the O/E frequency response of the PDs, representing optical-to-electrical conversion efficiency at different frequencies, is crucial and needs to be measured.

The O/E frequency response measurement is conventionally achieved by all optical methods, such as the optical heterodyne method [6], [7] and the optical pulse method [8]–[10]. The two methods feature ultrabroad bandwidth but suffer from low-frequency resolution and relatively complicated structures. Restricted by the low-frequency resolution, the advanced O/E devices for ultrahigh capacity optical communication are difficult to be fabricated, and the MWP-based technologies with ultrahigh resolution are hard to be enabled [11]. By combining fine microwave frequency sweeping and electrical-to-optical conversion, electrical spectrum analysis method [12], [13] and harmonic analysis method [14], [15] are developed and demonstrated, which feature high-frequency resolution. A sub-hertz frequency resolution is theoretically achievable if an ultranarrow linewidth laser and sufficient measurement points are employed. The electrical spectrum analysis method requires a relatively complicated electro-optic modulation, which not only introduces considerable nonlinearity error but also reduces the dynamic range. By adopting the two-tone modulation [16], the measurement accuracy together with dynamic range can be improved. Nevertheless, the limited working bandwidth of electro-optic modulators (EOMs) places a restriction on the O/E measurement bandwidth. To extend the measurement bandwidth, the harmonic analysis method is proposed, which has a doubled measurement bandwidth benefitting from the second harmonic component detection. Unfortunately, due to the limited extinction ratio of the EOMs, the optical carrier cannot be completely suppressed. The residual optical carrier would introduce the error together with the high-order sidebands induced by electro-optic nonlinearity.

In this article, an O/E frequency response measurement method with high-frequency resolution and broad measurement bandwidth is proposed and experimentally demonstrated. In the proposed O/E frequency response measurement method, a carrier-frequency-shifted optical double-sideband (ODSB) signal is produced by employing a dual-drive Mach-Zehnder modulator (DD-MZM) and stimulated Brillouin scattering (SBS). A PD under test converts the optical signal into a photocurrent. By detecting the generated frequency up- and down-conversion components, the O/E frequency responses in the low- and high-frequency regions are achieved. Then,

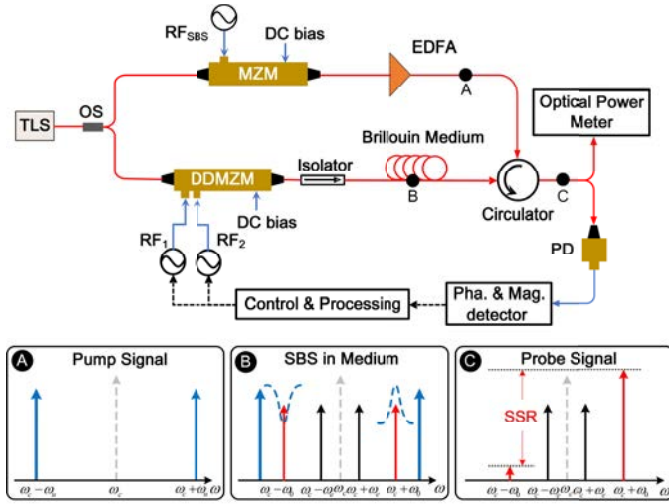


Fig. 1. Schematic block diagram of the proposed O/E frequency response measurement system. TLS: tunable laser source. OS: optical splitter. DD-MZM: dual-drive Mach-Zehnder modulator. MZM: Mach-Zehnder modulator. EDFA: erbium-doped fiber amplifier. PD: photodetector.

by stitching the two frequency responses together, a bandwidth doubled O/E frequency response is obtained. In an experiment, a commercial high-speed PD with a 3-dB bandwidth of 20 GHz is precisely characterized. The frequency resolution is set to 5.55 MHz, and a measurement bandwidth of 66.8 GHz (from 0.1 to 66.9 GHz) is achieved by using a 25-GHz DD-MZM.

## II. ANALYTICAL ANALYSIS

The schematic block diagram of the proposed O/E frequency response measurement method utilizing photonics-based frequency conversion is shown in Fig. 1. In the proposed method, a lightwave from a tunable laser source, serving as an optical carrier, is divided into two parts. In the upper branch, the optical carrier is modulated by an RF signal at a single-drive MZM. By setting the MZM at the minimum transmission point, a carrier-suppressed ODSB signal is produced. An erbium-doped fiber amplifier (EDFA) amplifies the ODSB signal. The amplified ODSB signal goes to a Brillouin medium through an optical circulator and serves as an optical pumping signal.

In the lower branch, a frequency-fixed RF signal and a frequency-swept RF signal are, respectively, applied to the two arms of a DD-MZM. By balancing the powers of the frequency-fixed and frequency-swept RF signals and properly setting the dc bias voltage, a carrier-suppressed ODSB signal is thus achieved, which is given by

$$E(t) = \frac{E_c}{\sqrt{2}} \exp[i\omega_c t + i\beta \sin(\omega_0 t) + i\pi] + \frac{E_c}{\sqrt{2}} \exp[i\omega_c t + i\beta \sin(\omega_e t + \Delta\phi)] \quad (1)$$

where  $E_c$  and  $\omega_c$  are, respectively, the magnitude and angular frequency of the optical carrier.  $\omega_0$  and  $\omega_e$  are the angular frequencies of the frequency-fixed and the frequency-swept RF signals, respectively, while  $\Delta\phi$  is the initial phase difference and  $\beta$  is the modulation index.

By carefully setting the RF powers, the DD-MZM operates at a small modulation index. In this case, the high-order sidebands induced by the modulation nonlinearity is small enough to be ignored. According to the Jacobi–Anger expansion, the expression of the output optical signal can be simplified as

$$E(t) = \frac{E_c}{\sqrt{2}} \exp(i\omega_c t) \{-J_{-1}(\beta) \exp[i(\omega_c - \omega_0)t] - J_1(\beta) \exp[i(\omega_c + \omega_0)t] + J_{-1}(\beta) \exp[i(\omega_c - \omega_e)t - i\Delta\phi] + J_1(\beta) \exp[i(\omega_c + \omega_e)t + i\Delta\phi]\} \quad (2)$$

where  $J_{\pm 1}(\cdot)$  is the  $\pm 1$ st-order Bessel function of the first kind.

Let the angular frequency of the RF signal be equal to the sum of  $\omega_0$  and the Brillouin frequency shift of the Brillouin medium. When the generated ODSB signal goes through the Brillouin medium, the  $-1$ st- and  $+1$ st-order sidebands generated by the frequency-fixed RF signal are, respectively, attenuated and amplified by the SBS. Hence, a carrier-frequency-shifted ODSB signal is obtained, which is

$$E_p(t) = \frac{E_c}{\sqrt{2}} \exp(i\omega_c t) \{-A(\omega_c - \omega_0) J_{-1}(\beta) \exp[i(\omega_c - \omega_0)t] - G(\omega_c + \omega_0) J_1(\beta) \exp[i(\omega_c + \omega_0)t] + J_{-1}(\beta) \exp[i(\omega_c - \omega_e)t - i\Delta\phi] + J_1(\beta) \exp[i(\omega_c + \omega_e)t + i\Delta\phi]\} \quad (3)$$

where  $G(\omega)$  and  $A(\omega)$  are the gain and absorption of the SBS stimulated by the optical pumping signal in the upper branch. With proper pumping power, a ratio of the gain and absorption larger than 30 dB is achievable. Thus, the attenuated  $-1$ st-order sideband is small enough to be ignored. The expression of the carrier-frequency-shifted ODSB signal can be simplified as

$$E_p(t) = \frac{E_c}{\sqrt{2}} \exp(i\omega_c t) \{-G(\omega_c + \omega_0) J_1(\beta) \exp[i(\omega_c + \omega_0)t] + J_{-1}(\beta) \exp[i(\omega_c - \omega_e)t - i\Delta\phi] + J_1(\beta) \exp[i(\omega_c + \omega_e)t + i\Delta\phi]\}. \quad (4)$$

A PD under test converts the carrier-frequency-shifted ODSB signal into a photocurrent, wherein the frequency down- and up-conversion components carry the O/E frequency responses in the low- and high-frequency regions, respectively. The electrical fields of the two components can be expressed by

$$i(\omega_0 - \omega_e) = -R(\omega_0 - \omega_e) \frac{E_c^2}{2} G(\omega_c + \omega_0) J_1^2(\beta) \exp(-i\Delta\phi) \quad (5)$$

$$i(\omega_0 + \omega_e) = -R(\omega_0 + \omega_e) \frac{E_c^2}{2} G(\omega_c + \omega_0) J_1^2(\beta) \exp(i\Delta\phi) \quad (6)$$

where  $R(\omega)$  is the O/E frequency response of the PD under test.

When the frequency-swept RF signal is suspended, the power of the frequency-shifted carrier can be measured

by an optical power meter, which is

$$P_c = \frac{E_c^2}{2} G^2 (\omega_c + \omega_0) J_1^2(\beta). \quad (7)$$

Similarly, the optical power of the frequency-swept +1st- and -1st-order sidebands can be obtained when the frequency-fixed RF signal is switched OFF

$$P_{\pm 1} = E_c^2 J_1^2(\beta). \quad (8)$$

According to (5)–(8), the O/E frequency responses can be achieved, which can be expressed by

$$R(\omega_0 - \omega_e) = \frac{\sqrt{2}|i(\omega_0 - \omega_e)|}{\sqrt{P_c P_{\pm 1}}} \quad (9)$$

$$R(\omega_0 + \omega_e) = \frac{\sqrt{2}|i(\omega_0 + \omega_e)|}{\sqrt{P_c P_{\pm 1}}}. \quad (10)$$

When sweeping  $\omega_e$  from dc to  $\omega_0$ , the O/E frequency responses over dc  $\sim \omega_0$  and  $\omega_0 \sim 2\omega_0$  are obtained according to (9) and (10). By stitching the two O/E frequency responses together, the O/E frequency response with a measurement bandwidth of  $2\omega_0$  is thus achieved, which is twice the sweeping range of the frequency-swept RF signal and the bandwidth of the EOM. It is worth noting that the measurement system is insensitive to the nonlinearity of the EOM. One reason is that the desired frequency up- and down-conversion components are only achieved by the two first-order sidebands and the frequency-shifted carrier. It is because the two RF signals are, respectively, modulated on the optical carrier and no high-order intermodulation sideband is generated. Another reason is that the measurement error induced by the high-order sidebands is small enough to be ignored due to the suppression of the even-order sidebands.

### III. EXPERIMENT AND DISCUSSION

An O/E frequency response measurement system based on the schematic block diagram shown in Fig. 1 is established, and an experiment is conducted. A 1550-nm lightwave produced by a narrow-linewidth laser (TeraXion PS-NLL-1550) is split into two branches. In the upper branch, an RF source (Agilent E8257D) provides a frequency-swept RF signal, and a single-drive 40-Gbps MZM (Fujitsu FTM7938EZ) biased at the minimum transmission point by using a modulator bias controller (PlugTech) serves as an EOM. An EDFA produced by Amonics Inc. amplifies the optical signal. In the lower branch, a four-port vector network analyzer (VNA, R&S ZVA67) produces a frequency-fixed RF signal and a frequency-swept RF signal, which are then injected into the two RF input ports of a 40-Gbps DD-MZM (Fujitsu FTM7937EZ) with a proper dc bias, respectively. A 20-km single-mode fiber (SMF) is used as the SBS medium. A commercial high-power PD owning a 3-dB working bandwidth of 20 GHz (Discovery Semiconductors Inc. DSC40S) is served as the device under test. The VNA receives the frequency up- and down-conversion components and then extracts the magnitude information. An optical multiport power meter (Agilent N7744A) measures the optical powers

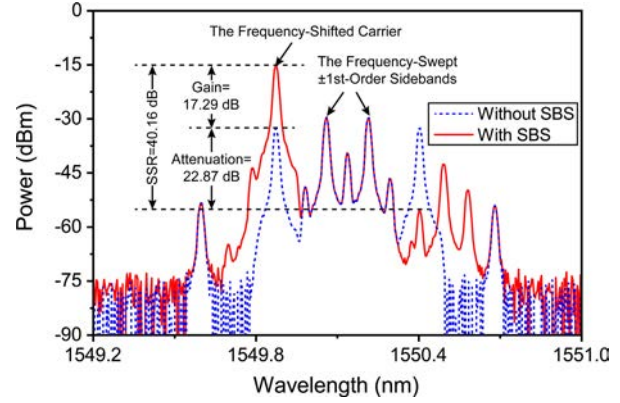


Fig. 2. Optical spectra of the carrier-suppressed and the carrier-frequency-shifted ODSB signals.

of the frequency-swept first-order sidebands at different frequencies and the frequency-shifted optical carrier. An optical spectrum analyzer (OSA, Yokogawa AQ6370C) monitors and records the optical spectra with a frequency resolution of 1.6 pm.

Fig. 2 shows the optical spectra of the carrier-suppressed ODSB signal and the carrier-frequency-shifted ODSB signal achieved by the SBS processing. The frequency of the frequency-fixed RF signal is set to 33.5 GHz, which is half of the measurement bandwidth limited by the bandwidth of the VNA. The frequency-swept RF signal is set to a fixed frequency of 10 GHz. The two RF signals have an equal power of 7 dBm, so that the original optical carrier is suppressed by applying a proper dc bias voltage. The generated carrier-suppressed ODSB signal is represented by the blue dashed line in Fig. 2. By setting the frequency spacing of the two frequency-swept RF signals in the upper and low branches exactly equal to the Brillouin frequency shift of the 20-km SMF (e.g., 10.67 GHz in the experiment), a carrier-frequency-shifted ODSB signal is achieved, as represented by the red solid line in Fig. 2. Considering 17.29-dB gain and 22.87-dB attenuation of the SBS in the SMF, the amplified +1st-order sideband is 40.16-dB larger than the -1st-order sideband. Due to the limited extinction ratio of the MZM (typ.  $\sim 20$  dB), the original optical carrier is incompletely suppressed, which is 10.14 and 24.49 dB smaller than the two frequency-swept first-order sidebands and the frequency-shifted carrier. In the optical power measurement, the residual original carrier introduces 4.85% and 0.36% errors, which results in a 2.58% error in the measured response. The measurement error can be greatly reduced, if a high-extinction-ratio MZM is used. It should be noted that the optical pumping signal introduces the Rayleigh backscattering and Brillouin backscattering in the SBS processing. Fortunately, the backscattering signals introduce no error in the desired components and 0.19% error in the frequency-shifted carrier power measurement due to the relatively small powers.

Fig. 3 shows the measured O/E frequency responses of the commercial high-speed PD by the proposed measurement method and a commercial instrument. As can be seen from Fig. 3(a), by detecting the frequency down-conversion

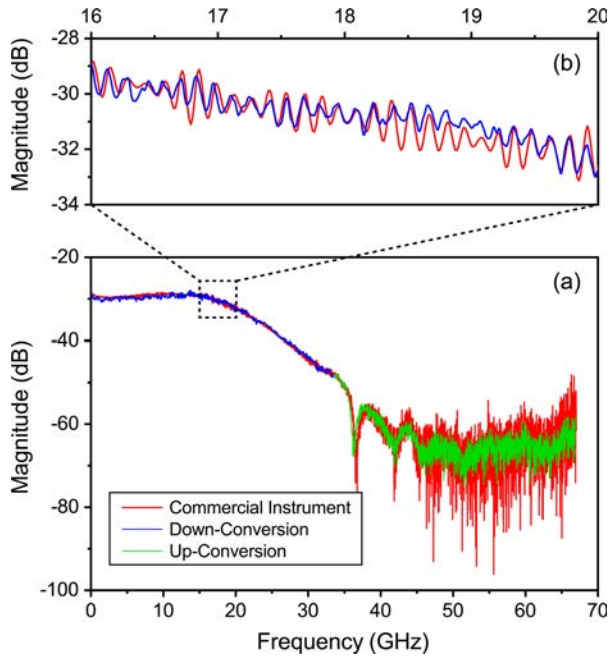


Fig. 3. (a) O/E frequency responses measured by the proposed method and the commercial instrument. (b) Zoomed-in view of the O/E frequency responses.

component, the O/E frequency response from 0.1 to 33.4 GHz (blue lines) is obtained. Since there are 6001 measurement points in a frequency sweeping range of 33.3 GHz, the frequency resolution is 5.55 MHz. A sub-kilohertz resolution is potentially available in theory if a sub-hertz-linewidth laser source is employed and sufficient measurement points are adopted. Similarly, the O/E frequency response from 33.6 to 66.9 GHz (green line) with a frequency resolution of 5.55 MHz is achieved by detecting the frequency up-conversion component. Benefitting from the accurate frequency of the microwave signal, the two measured responses are precisely stitched, and an O/E frequency response with a doubled measurement bandwidth of 66.8 GHz (from 0.1 to 66.9 GHz) is obtained.

As a comparison, the O/E frequency response obtained by the lightwave component analyzer (Keysight N4373D) is represented by red lines in Fig. 3. The O/E frequency response achieved by the proposed method is coincident with that measured by the commercial instrument. The two measured O/E frequency responses have the same up and down in the low-frequency region shown in Fig. 3(b). The slight difference within  $\pm 0.65$  dB can be observed between the responses measured by the two methods, because the relative O/E measurement uncertainty of the lightwave component analyzer at 1550 nm is  $\pm 0.8$  dB [17] and the measurement accuracy of the VNA used in the experiment is  $\pm 0.3$  dB. At high frequencies beyond 35 GHz, the proposed method has a better noise performance than the commercial instrument. As can be seen, an optical-to-electrical conversion loss up to 70 dB is measurable. Considering the  $\sim 20$ -dB gain, a dynamic range as large as 90 dB is achievable. It is worth mentioning that, by increasing the RF powers, the noise performance and the dynamic range can be further improved.

#### IV. CONCLUSION

In conclusion, an O/E frequency response measurement method utilizing photonics-based frequency conversion is proposed and experimentally demonstrated. The proposed measurement method is attractive by its high-frequency resolution and doubled measurement bandwidth. In the experiment, the commercial high-speed PD is characterized. The O/E frequency response in a bandwidth of 66.8 GHz (from 0.1 to 66.9 GHz) is obtained by using a 25-GHz DD-MZM. The measurement result coincides with that measured by the commercial instrument.

#### REFERENCES

- [1] N. Pleros, K. Vyrsokinos, K. Tsagkaris, and N. D. Tselikas, "A 60 GHz radio-over-fiber network architecture for seamless communication with high mobility," *J. Lightw. Technol.*, vol. 27, no. 12, pp. 1957–1967, Jun. 15, 2009.
- [2] D. Zhu, T. Du, and S. Pan, "A coupled optoelectronic oscillator with performance improved by enhanced spatial hole burning in an erbium-doped fiber," *J. Lightw. Technol.*, vol. 36, no. 17, pp. 3726–3732, Sep. 1, 2018.
- [3] R. Waterhouse and D. Novack, "Realizing 5G: Microwave photonics for 5G mobile wireless systems," *IEEE Microw. Mag.*, vol. 16, no. 8, pp. 84–92, Sep. 2015.
- [4] S. Pan and Y. Zhang, "Microwave photonic radars," *J. Lightw. Technol.*, vol. 38, no. 19, pp. 5450–5484, Oct. 1, 2020.
- [5] S. Pan, X. Ye, Y. Zhang, and F. Zhang, "Microwave photonic array radars," *IEEE J. Microw.*, vol. 1, no. 1, pp. 176–190, Jan. 2021.
- [6] T. S. Tan, R. L. Jungerman, and S. S. Elliott, "Optical receiver and modulator frequency response measurement with a Nd: YAG ring laser heterodyne technique," *IEEE Trans. Microw. Theory Techn.*, vol. 37, no. 8, pp. 1217–1222, Aug. 1989.
- [7] N. H. Zhu, J. M. Wen, H. S. San, H. P. Huang, L. J. Zhao, and W. Wang, "Improved optical heterodyne methods for measuring frequency responses of photodetectors," *IEEE J. Quantum Electron.*, vol. 42, no. 3, pp. 241–248, Mar. 2006.
- [8] N. G. Paulter, A. J. A. Smith, D. R. Larson, T. M. Souders, and A. G. Roddie, "NIST-NPL interlaboratory pulse measurement comparison," *IEEE Trans. Instrum. Meas.*, vol. 52, no. 6, pp. 1825–1833, Dec. 2003.
- [9] D. R. Larson, N. G. Paulter, and D. I. Bergman, "Pulse parameter dependence on transition occurrence instant and waveform epoch," *IEEE Trans. Instrum. Meas.*, vol. 54, no. 4, pp. 1520–1526, Aug. 2005.
- [10] D. F. Williams *et al.*, "Covariance-based uncertainty analysis of the NIST electrooptic sampling system," *IEEE Trans. Microw. Theory Techn.*, vol. 54, no. 1, pp. 481–491, Jan. 2006.
- [11] T. Qing, S. Li, Z. Tang, B. Gao, and S. Pan, "Optical vector analysis with attometer resolution, 90-dB dynamic range and THz bandwidth," *Nature Commun.*, vol. 10, no. 1, pp. 1–9, Nov. 2019.
- [12] S. Zhang *et al.*, "Self-calibrated microwave characterization of high-speed optoelectronic devices by heterodyne spectrum mapping," *J. Lightw. Technol.*, vol. 35, no. 10, pp. 1952–1961, May 15, 2017.
- [13] M. Yoshioka, S. Sato, and T. Kikuchi, "A method for measuring the frequency response of photodetector modules using twice-modulated light," *J. Lightw. Technol.*, vol. 23, no. 6, pp. 2112–2117, Jun. 1, 2005.
- [14] B. H. Zhang *et al.*, "Development of swept frequency method for measuring frequency response of photodetectors based on harmonic analysis," *IEEE Photon. Technol. Lett.*, vol. 21, no. 7, pp. 459–461, Apr. 3, 2009.
- [15] K. Inagaki, T. Kawanishi, and M. Izutsu, "Optoelectronic frequency response measurement of photodiodes by using high-extinction ratio optical modulator," *IEICE Electron. Exp.*, vol. 9, no. 4, pp. 220–226, 2012.
- [16] H. Wang *et al.*, "Two-tone intensity-modulated optical stimulus for self-referencing microwave characterization of high-speed photodetectors," *Opt. Commun.*, vol. 373, pp. 110–113, Aug. 2016.
- [17] (2017). *Keysight N4373D Lightwave Component Analyzer User's Guide*. Keysight Technologies, Manual Part Number 4373D-90A02. [Online]. Available: <https://literature.cdn.keysight.com/litweb/pdf/4373D-90A02.pdf>

**Min Xue** received the B.S. and Ph.D. degrees in electronics engineering from the Nanjing University of Aeronautics and Astronautics, Nanjing, China, in 2011 and 2016, respectively.

He joined the College of Electronic and Information Engineering, Nanjing University of Aeronautics and Astronautics, in 2016, where he is currently a member of the Key Laboratory of Radar Imaging and Microwave Photonics, Ministry of Education. He serves as the Publication Co-Chair of the *IEEE International Topical Meeting on Microwave Photonics* in 2017. His research interests include photonic microwave measurement and metrology, optical fiber sensors, and integrated microwave photonics.

Dr. Xue was a recipient of the Gold Medal with congratulations of the jury in the 45th International Exhibition of Inventions of Geneva in 2017 and the “Hong Kong Scholars” in 2018.

**Minghui Lv** received the B.S. and M.S. degrees in electronics engineering from the Nanjing University of Aeronautics and Astronautics, Nanjing, China, in 2018 and 2021, respectively.

His research interests include electrooptic and optic-electro devices measurement.

**Qi Wang** received the B.S. degree in electronics engineering from the Nanjing University of Aeronautics and Astronautics, Nanjing, China, in 2019, where she is currently pursuing the M.S. degree with the Key Laboratory of Radar Imaging and Microwave Photonics, Ministry of Education.

**Beibei Zhu** received the B.S. degree in electronics engineering from the Nanjing University of Aeronautics and Astronautics, Nanjing, China, in 2013, where she is currently pursuing the Ph.D. degree with the Key Laboratory of Radar Imaging and Microwave Photonics, Ministry of Education.

Her research interests include photonic microwave generation, transmission, and measurement.

**Changyuan Yu** (Senior Member, IEEE) received the Ph.D. degree in electrical engineering from the University of Southern California, Los Angeles, CA, USA, in 2005.

He was a Visiting Researcher with the NEC Laboratories America, Princeton, NJ, USA in 2005. He joined as a Faculty with the National University of Singapore (NUS), Singapore, in December 2005, where he served as the Founding Leader for the Photonic System Research Group, Department of Electrical and Computer Engineering. He was also a Joint Senior Scientist with the Institute for Infocomm Research (I2R), Agency for Science, Technology and Research (A\*STAR), Singapore. In December 2015, he joined The Hong Kong Polytechnic University as a tenured Associate Professor with the Department of Electronic and Information Engineering. He also continues as an adjunct Associate Professor with NUS. He has authored or coauthored six book chapters, and 400+ journal articles and conference papers (82 keynote/invited, including OFC2012 in USA). His research focuses on photonic devices, subsystems, optical fiber communication and sensor systems, and biomedical instruments.

Dr. Yu group won six best paper awards in conferences and the championship in biomedical area in the Third China Innovation and Entrepreneurship Competition in 2014.

**Shilong Pan** (Senior Member, IEEE) received the B.S. and Ph.D. degrees in electronic engineering from Tsinghua University, Beijing, China, in 2004 and 2008, respectively.

From 2008 to 2010, he was a “Vision 2010” Post-Doctoral Research Fellow with the Microwave Photonics Research Laboratory, University of Ottawa, Ottawa, ON, Canada. He joined the College of Electronic and Information Engineering, Nanjing University of Aeronautics and Astronautics, Nanjing, China, in 2010, where he is currently a Full Professor and an Executive Director of the Key Laboratory of Radar Imaging and Microwave Photonics, Ministry of Education. He has authored or coauthored over 430 research articles, including more than 240 articles in peer-reviewed journals and 190 articles in conference proceedings. His research has focused on microwave photonics (MWP), which includes optical generation and processing of microwave signals, photonic microwave measurement, and integrated MWP.

Dr. Pan is a fellow of OSA, SPIE, and IET. He was selected as an IEEE Photonics Society Distinguished Lecturer in 2019. He is currently an Associate Editor of *Electronics Letters*, a Topical Editor of *Chinese Optics Letters*, and a Technical Committee Member of the IEEE MTT-3 Microwave Photonics. He served as the Chair for a number of international conferences, symposia, and workshops, the TPC Chair for the International Conference on Optical Communications and Networks in 2015, and the TPC Co-Chair for the IEEE International Topical Meeting on Microwave Photonics in 2017.